Modeling versus Accuracy in EEG and MEG Data

John C. Mosher, Richard M. Leahy, Ming-xiong Huang, Michael E. Spencer

Los Alamos National Laboratory
Group P-21 MS D454
Los Alamos, NM 87545
mosher@LANL.Gov, (505) 665-2175

Signal & Image Processing Institute
University of Southern California
EEB 400 MS 2564
Los Angeles, CA 90089-2564

Signal Processing Solutions
807 Avenue A
Redondo Beach, CA 90277-4815

Los Alamos Technical Report No. LA-UR-97-3181

Modeling versus Accuracy in EEG and MEG Data

Mosher J.C.[1], Leahy R.M.[2], Huang M.[1], Spencer M.E.[3]

[1]Los Alamos National Laboratory, Los Alamos, New Mexico USA
[2]University of Southern California, Los Angeles, California USA
[3]Signal Processing Solutions, Redondo Beach, California USA

Introduction

The widespread availability of high-resolution anatomical information has placed a greater emphasis on accurate electroencephalography and magnetoencephalography (collectively, E/MEG) modeling. A more accurate representation of the cortex, inner skull surface, outer skull surface, and scalp should lead to a more accurate forward model and hence improve inverse modeling efforts. We examine a few topics in this paper that highlight some of the problems of forward modeling, then discuss the impacts these results have on the inverse problem.

We begin by assuming a perfect head model, that of the sphere, then show the lower bounds on localization accuracy of dipoles within this perfect forward model. For more realistic anatomy, the boundary element method (BEM) is a common numerical technique for solving the boundary integral equations. For a three-layer BEM, the computational requirements can be too intensive for many inverse techniques, so we examine a few simplifications. We quantify errors in generating this forward model by defining a regularized percentage error metric. We then apply this metric to a single layer boundary element solution, a multiple sphere approach, and the common single sphere model. We conclude with an MEG localization demonstration on a novel experimental human phantom, using both BEM and multiple spheres.

Methods

Cramer-Rao Lower Bounds

Even if we know our forward head and source model precisely, noise prevents us from exactly determining the location of a dipole. Our inverse estimation process will make some error in locating the dipole, an error often characterized by its mean (bias) and variance. No unbiased estimator can have a lower error variance than that established by the Cramer-Rao lower bound (CRLB). In [1], we presented this formal analysis of dipole localization error, for both EEG and MEG, assuming that the forward model was perfectly known. The CRLBs were generated for the cases of one and two dipoles and for varying densities of sensor array patterns. The MEG sensors were assumed in [1] to be magnetometers. In this paper, we present the CRLBs for the case of axial versus planar gradiometers, both as a demonstration of the flexibility of the CRLB in performing system analyses, as well as establishing some fundamental error bounds useful for inverse problem discussions.

Regularized Percentage Error

We define the regularized percentage (RP) error as follows. We assume that a particular head model approach has generated a gain matrix designated as A for a particular dipole location. We assume a competing head model has generated a similar gain matrix B for the same dipole location. For a particular dipole moment q, the forward field observed at N sensors would be $a = Aq$ or $b = Bq$; see [2] for a more complete review of this gain matrix model. Our problem is to quantify the difference between the two observed patterns in a meaningful manner. We might calculate the sum squared error between the two vectors, denoted as $\|a - b\|_2^2$; however, this error quantity is generally more useful if scaled by the field magnitude, $\|a - b\|_2^2 / a^2$. Similar error metrics have been widely used by other E/MEG researchers in evaluating head models. In each of these instances, the error has been scaled by the field value in order to achieve a figure of merit; however, these measures do not address the problem of field values too small to be of concern. For instance, a radial dipole inside a perfect sphere has zero external magnetic field, and in a realistic head shape, the external field can be expected to be quite small. In these instances, the error measures above will yield widely varying figures of merit, yet in the inverse problem these small field difference will be almost surely dominated by noise. Thus the differences between these models should be of no consequence, and the figure of merit should be adjusted accordingly. A second problem with these error definitions is that they apply only to the specific dipole orientation q used to generate the forward fields represented by a and b.

A more meaningful calculation would be the best and worst error over all possible dipole orientations, with respect to an anticipated noise level. Conceptually, we first simply modify the existing error functions to account for an anticipated noise variance σ^2, i.e., our metric might be $\|a - b\|_2^2 / (a^2 + \sigma^2)$. Thus small total field values a are "regularized" by σ^2. Second, we relax the dependence of the analysis on the dipole moment by computing the error $\|Aq - B\hat{q}\|_2^2$, where $\hat{q}$ is the dipole orientation that minimizes this error for a particular q. Accounting for the scale factor and noise regularizer, we can then, in a manner analogous to our MUSIC presentation in [2], maximize or minimize over all q using a *generalized eigenanalysis*, succinctly expressed and readily calculated in MATLAB as

$$e_{\mathrm{RP}} = \mathrm{eig}\left(A^T P_B^\perp A, \; A^T A + \frac{N}{SNR} I\right) \qquad (1)$$

which we denote as the *regularized percentage error*, where N is the number of sensors, and $P_B^\perp$ is a projection

operator for the subspace orthogonal to **B** . The signal to noise ratio *SNR* is the ratio of the square of the dipole intensity to the variance of the noise at each sensor, as we defined in [1]. The key property of this metric is that it directly reflects localization ability since we can use it to find the *worst error* over all possible dipole orientations and locations in the head. Furthermore, the metric includes the effects of noise. We will use this in our evaluation of head models described below.

Boundary Elements and Multiple Sphere Head Models

The routine use of boundary element method (BEM) models is limited by their high computational cost (up to three orders of magnitude greater than that of the spherical model). Models based on a single set of concentric spheres, however, do not well represent the shape of the human head or the impact of the associated volume currents. A compromise between these can be realized by locally varying the centers and radii of the spherical model to match the local curvature of the head. Intuitively, as in [3], such a model could be fitted by observing the local curvature of the scalp and skull surfaces and generating a least-square fit of a sphere to this local surface. We have developed a modified form of this locally fitted sphere method. Each sensor is assigned its own best fitting sphere, but the least-squares fit is weighted using the lead fields that such a sensor would produce in a spherical model. The spherical lead fields are calculated at the scalp or skull surfaces, then the sphere center iteratively adjusted until the weighted least-squares error between the spherical model and the anatomical surface is minimized. We refer to this approach as the *weighted multi-sphere (*WMS) head model [4].

We performed a preliminary computer evaluation using the regularized percentage (RP) error. We extracted a three-layer BEM model from an MRI, as well as a smoothed representation of the cortical surface. A full three-layer BEM numerical computation was used as the "gold standard" against which to test the other techniques. In Fig. 1, we show the RP error for the WMS (b) and the single sphere (c) versus the three-layer BEM. The image intensities shown on each of the rendered cortical surfaces show the *worst* case RP error (according to scale on right) over all possible dipole orientations at each point on the cortical surface. We also present the RP error for a one-layer BEM, which uses only the inner skull surface. As also supported by the observations in [5], the one-layer BEM model (a) is quite adequate for MEG, and this study suggests that the WMS head model will also be adequate, yet several orders of magnitude faster to compute.

The WMS head model is easily adapted to other specialized shapes, such as presented in [6]. The novelty of our approach is the iterative calculation of the lead fields to use as the weighting factor in the spherical fitting. Our application of the RP error focuses the design issue on the portions of the forward model relevant to inverse fitting and allows rapid calculation of thousands of dipole locations, at each location automatically extracting the best and worst dipole orientations.
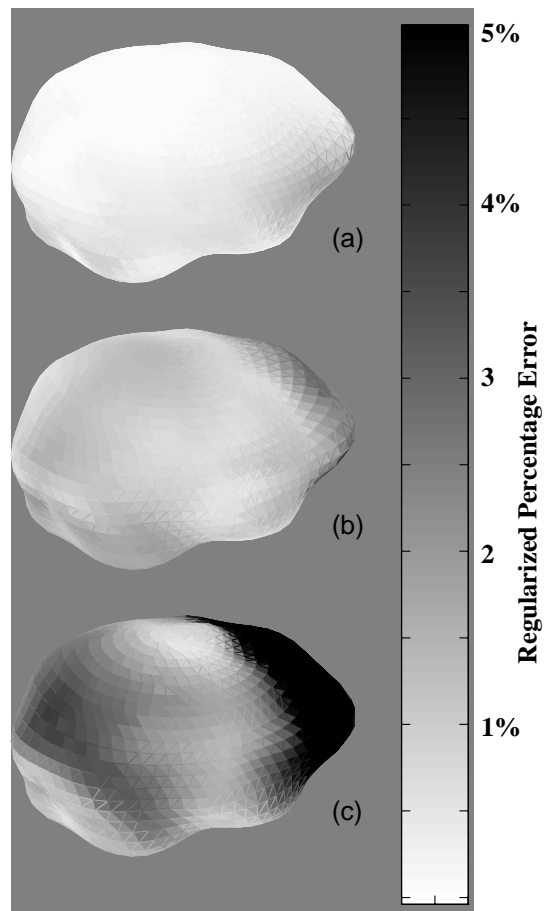

Fig. 1: From [4], the regularized percentage (RP) error between a full three-layer MEG BEM model and (a) a one-layer (inner skull) BEM model; (b) our proposed WMS model; and (c) the conventional single sphere model. The study was for a simulated 127 magnetometer system, a 10 nA-m dipole source and zero-mean Gaussian noise with a 10 fT standard deviation. We observe the significant error of the single sphere (c) in modeling the forward regions of the head, while the WMS head model (b) only generates errors of a few percent in this region.

Experimental Phantom

To generate realistic data sets for both EEG and MEG, we recently completed the construction and preliminary testing of a human skull phantom [7]. The sources are 32 coaxial wires entering through the base of the skull, and a source connector is attached to the driver electronics, also custom built for this phantom. Forty layers of NaCl-doped modeling latex were applied to the upper 2/3 of the skull to resemble a scalp layer and EEG electrodes attached, as shown in Fig. 2. A conductive gelatin was formed by doping a mixture with NaCl. The human skull was then immersed in hot solution of the gelatin, ensuring that the diploic space of the skull was thoroughly impregnated. The result is a homogeneous "brain" mass, in which the coaxial sources inject current through the tips and return the current through the shields. The ground of each source was optically isolated (greater than 100 dB separation between dipoles), ensuring that the sources appeared to both EEG and MEG as current dipole sources. Each dipole is independently programmable through a PC interface. Careful

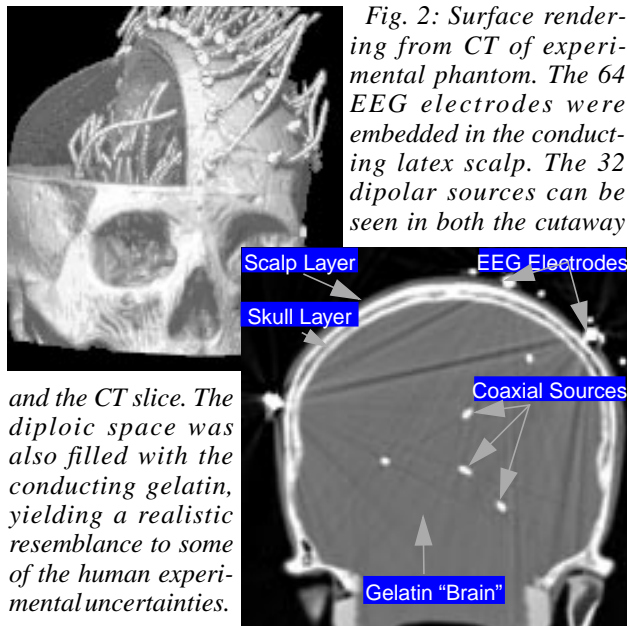**Los Alamos Technical Report No. LA-UR-97-3181**   **August 08, 1997**

Fig. 2: Surface rendering from CT of experimental phantom. The 64 EEG electrodes were embedded in the conducting latex scalp. The 32 dipolar sources can be seen in both the cutaway

and the CT slice. The diploic space was also filled with the conducting gelatin, yielding a realistic resemblance to some of the human experimental uncertainties.

restrictions to non-ferrous materials made this phantom compatible with the MEG sensor array. As shown in Fig. 2, the CT images were rendered and the images closely examined to extract the precise position of both the EEG electrodes and the coaxial current sources.

Results

Axial versus Planar Gradiometers

Fig. 3 presents the Cramer-Rao lower bounds, as discussed in [1], comparing the theoretical lower bound on error performance of a simulated axial gradiometer array with that of a planar gradiometer array. To hold constant the other parameters of consideration, both arrays were simulated on a 30 mm spaced grid on a 120 mm virtual sphere. The error analysis was performed for regions at least 20 mm from the array, i.e. at radii less than 100 mm. The isocontour lines represent regions within a perfect spherical head model that yield the same error performance, here expressed as the scalar standard deviation in mm for estimating a single dipole's location. The bottom figure in Fig. 3 is the difference between the two systems. Very near the surface, the performances are nearly identical, with less than 1 mm difference in standard deviations from radii of 70 mm to 100 mm. At increasing depths, we see the axial system outperforming the planar, but over a wide range of depths this difference may not be significant.

Phantom Dipole Localization

We extracted the inner skull, outer skull, and scalp surfaces from the CTs of the phantom and tessellated them for forward modeling in a BEM code. We present here preliminary results of our single-shell MEG BEM head model and analysis of our proposed WMS head model. Fig. 4 shows the scalar distance error between the dipoles as located in our CT images and the dipoles as found in single dipole fits of MEG data acquired in the Neuromag-122. The dashed lines show most of the errors were within
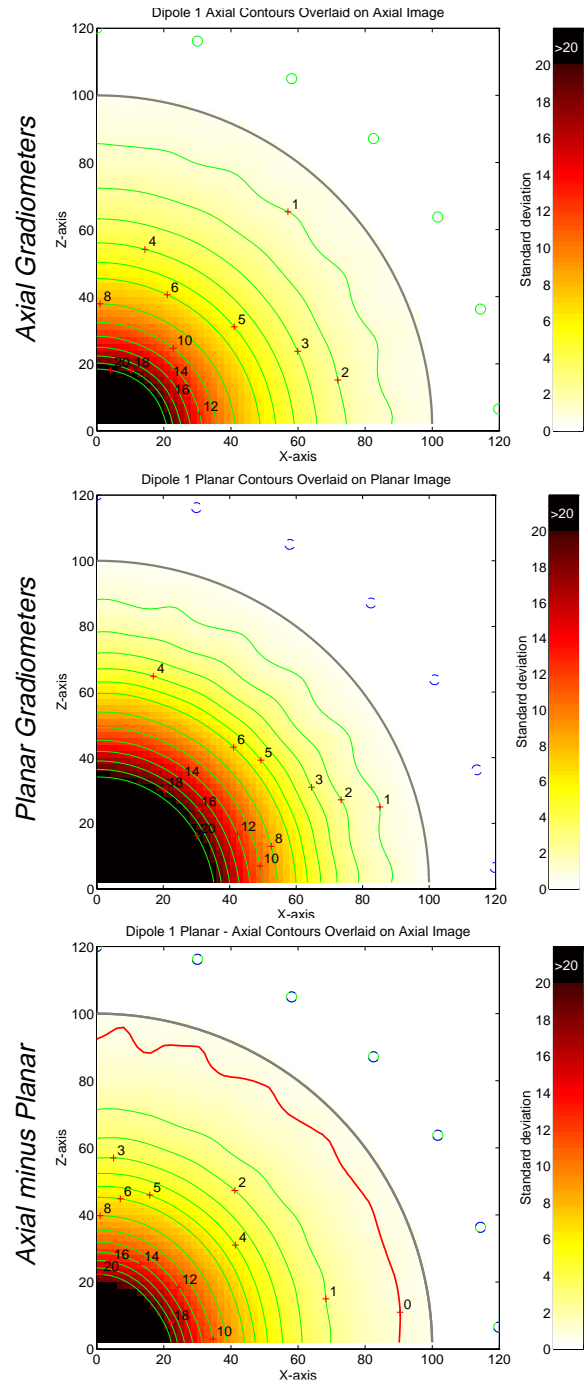

Fig. 3: Cramer-Rao Lower Bounds, for 152 sensor sites, all units are std. dev. in mm. The variations in the isocontours near the surface arise from the spatial sampling of the array. The noise is considered to be spatially and temporally white with a standard deviation of 10 fT, and the dipole intensity was held constant at 10 nA-m. The CRLB variances scale inversely proportional to the SNR, where SNR is defined below (1).

6 mm. To account for possible registration errors, we performed a global translation and rotation to the solution set, yielding a small improvement in the errors, as indicated by the solid lines in Fig. 4. We are in the process of re-registering all of the data, but this first look is very encouraging, since our CT images had a 2 mm axial slice thickness, and this initial BEM search was quantized to 2 mm. Fig. 5 illustrates the same processing, but using the WMS model at a fraction of the computational time of the BEM. The
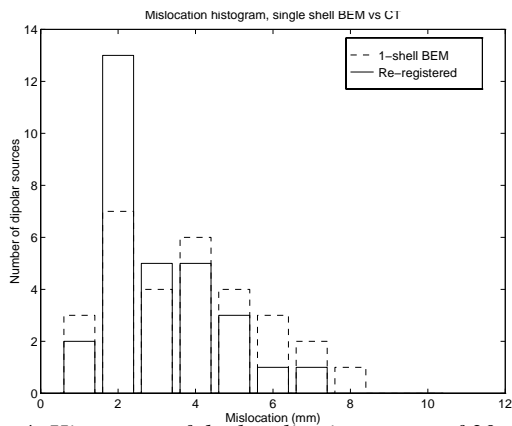
Fig. 4: Histogram of the localization errors of 30 single dipole sources in the human skull phantom, using a single layer BEM. We observe that 15 of the re-registered dipoles were within 2 mm of their corresponding CT locations.
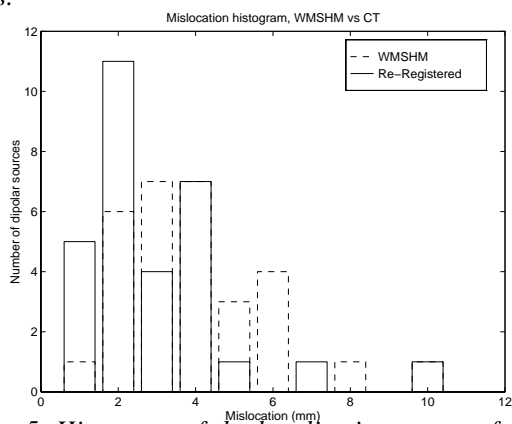

Fig. 5: Histogram of the localization errors of same dipoles as in Fig. 4, using instead a WMS approximation for the forward model, and again re-registering. The WMS model is calculated at a fraction of the computational cost of the BEM, with nearly the same localization performance.

same probable registration error was again noted, and we see that the mis-location errors are comparable to the BEM and quite small. Two of the 32 dipoles were omitted as outliers from this first look.

The SNR in this phantom study was approximately four times that of the simulation study presented in Fig. 3, therefore halving the CRLB standard deviations. Most of the dipole sources were about 50-70 mm from the array. If we ignore the head modeling errors of the phantom, we see that our localization errors are consistent with the bounds of Fig. 3.

Discussion

The WMS head model represents a markedly faster computational technique for calculating the forward model. The RP analysis suggests the differences are minor compared to the noise we might anticipate under experimental conditions, and the phantom localization results support this alternative forward model technique. We are presently applying the same approaches to EEG models.

In this brief paper, we have emphasized results with a single dipole model. As we showed in [1], however, the

CRLBs can rapidly increase for two or more dipoles placed as close as a few centimeters. We suggest that this fundamental localization error has far greater consequences on inverse procedures than the sensor differences and forward modeling errors we have presented here.

The relatively recent and rapidly widespread application of function magnetic resonance imaging (fMRI) for functional brain imaging studies has placed greater emphasis on the utility of electrophysiological data as a complement to hemodynamic data. A common suggestion is to constrain the E/MEG data with the locations found in fMRI, in order to extract the exquisite temporal resolution the E/MEG data represent. Our CT-based phantom anatomical images are allowing us to test such "fusion" assumptions under experimental conditions more controlled than fMRI. Even in the simple example of this paper, we already observe registration issues in combining anatomical information. The fMRI and E/MEG fusion of human data will be even more complicated, because the location of hemodynamic foci may not necessarily correspond with those of electrophysiological foci, and sources may be "silent" in either modality, thus altering the temporal data modeling.

References

[1] Mosher JC, Spencer ME, Leahy RM, Lewis PS, 1993, "Error bounds for EEG and MEG dipole source localization," *Electro clin Neurophysiology*, vol. 86, pp. 303-321.

[2] Mosher JC, Lewis PS, and Leahy RM, 1992, "Multiple dipole modeling and localization from spatio-temporal MEG data," *IEEE Trans. Biomedical Eng*, 39:541 - 557.

[3] Ilmoniemi RJ, Hamalainen MS, Knuutila J, 1985, "The forward and inverse problems in the spherical model," in *Biomagnetism: Applications and Theory*, eds Weinberg, Stroink, and Katila, Pergamon: New York, pp. 278-282.

[4] Huang M, Mosher JC, "A novel head model for the MEG forward problem: BEM accuracy with only spherical model complexity," *Neuroimage,* vol. 5, no. 4, May 1997, p. S441.

[5] Hämäläinen MS, and Sarvas J, 1989, "Realistic conductivity geometry model of the human head for interpretation of neuromagnetic data," *IEEE Trans. Biomed. Eng.*, vol 36, pp. 165 - 171.

[6] Cuffin BN, Cohen D, "Magnetic fields of a dipole in special volume conductor shapes," *IEEE Trans. Biomed. Eng.*, vol BME-24, July 1977, pp. 372–381.

[7] Spencer ME, Leahy RM, and Mosher JC, "A Skull-Based Multiple Dipole Phantom for EEG and MEG Studies," In Aine, Flynn, Okada, Stroink, Swithenby, and Wood (Eds.) *Biomag96: Advances in Biomagnetism Research*, Springer-Verlag, New York, 1997 (in press).

Acknowledgments